

UCRL-18184

cy. 2

University of California  
Ernest O. Lawrence  
Radiation Laboratory

TWO-WEEK LOAN COPY

*This is a Library Circulating Copy  
which may be borrowed for two weeks.  
For a personal retention copy, call  
Tech. Info. Division, Ext. 5545*

A SEMI-QUANTITATIVE MODEL OF POP-IN BEHAVIOR

W. W. Gerberich, P. L. Key and E. R. Parker

April 1968

RECEIVED  
LAWRENCE  
RADIATION LABORATORY

JUN 1 1968

LIBRARY AND  
DOCUMENTS SECTION

Berkeley, California

UCRL-18184  
cy. 2

## **DISCLAIMER**

This document was prepared as an account of work sponsored by the United States Government. While this document is believed to contain correct information, neither the United States Government nor any agency thereof, nor the Regents of the University of California, nor any of their employees, makes any warranty, express or implied, or assumes any legal responsibility for the accuracy, completeness, or usefulness of any information, apparatus, product, or process disclosed, or represents that its use would not infringe privately owned rights. Reference herein to any specific commercial product, process, or service by its trade name, trademark, manufacturer, or otherwise, does not necessarily constitute or imply its endorsement, recommendation, or favoring by the United States Government or any agency thereof, or the Regents of the University of California. The views and opinions of authors expressed herein do not necessarily state or reflect those of the United States Government or any agency thereof or the Regents of the University of California.

Submitted to The National  
Symposium on Fracture Mechanics,  
June 17-19, 1968  
Lehigh University, Bethlehem, Pa.

UCRL-18184  
Preprint

UNIVERSITY OF CALIFORNIA  
Lawrence Radiation Laboratory  
Berkeley, California  
AEC Contract No. W-7405-eng-48

A SEMI-QUANTITATIVE MODEL OF POP-IN BEHAVIOR

W. W. Gerberich, P. L. Key and E. R. Parker

April 1968

A SEMI-QUANTITATIVE MODEL OF POP-IN BEHAVIOR

W. W. Gerberich, P. L. Key and E. R. Parker

Inorganic Materials Research Division, Lawrence Radiation Laboratory,  
Department of Mineral Technology, College of Engineering,  
University of California, Berkeley, California

ABSTRACT

The complex material behavior associated with multiple pop-in phenomena has been treated with some degree of success. For pop-in length, the analysis considers an effective load reduction at the crack front due to plastic deformation. The effective stress intensity factor is decreased by the plastic deformation while it is increased by the length of pop-in,  $l$ . Due to these competing effects, the stress intensity,  $K$ , first increases and then decreases with increasing  $l$ . The point at which the effective  $K$  reduces back to the initial  $K$  defines  $l$ .

For a second or third pop-in, the stress intensity increment,  $\Delta K$ , between pop-ins is interpreted in terms of a changing fracture criterion (plane strain to plane stress) and the crack-tip blunting that occurs with increasing stress intensity. Although semi-quantitative in nature, these analyses do predict the experimentally observed increase in  $l$  and decrease in  $\Delta K$  associated with increasing  $K$ . The limits of these models provide additional insight into fracture behavior.

- a) As  $l \rightarrow 0$ : A geometrical lower bound for pop-in behavior is hypothesized.
- b) As  $\Delta K \rightarrow 0$ : The critical stress intensity factor at any particular thickness is given thus allowing establishment of the fracture-mode transition curve.

## INTRODUCTION

Recently, some evidence<sup>(1)</sup> on pop-in crack extension in plastics has revealed details of the pop-in shape as well as its relationship to the plastic zone surrounding it. These data suggested that there might be some relationship between the length of pop-in and the plastically deformed region surrounding it. Equally interesting pop-in phenomena<sup>(2)</sup> were obtained on an aluminum alloy wherein multiple pop-ins were observed. That is, about four pop-ins were commonly encountered at increasing stress intensity levels in a single test before failure. These data indicated that pop-in length was affected by the magnitude of applied stress intensity. Also, there appeared to be some stress-intensity increment required to initiate a second pop-in after the first.

These results provided impetus to formulate a semi-quantitative model for pop-in behavior which might explain some of the experimental observations. Specifically, answers to the following questions were desired.

- (1) Once a crack starts, why does it stop?
- (2) What governs the length of pop-in?
- (3) Why can a single specimen have more than one pop-in?
- (4) Are there geometrical or loading effects on the stress intensity increment required to produce a second or third pop-in?

## POP-IN LENGTH CONSIDERATION

First, consider what happens when a pop-in step occurs. The load during the sudden extension of the crack should remain constant or decrease depending on the stiffness of the testing machine. Thus, one might envision that the reason the crack stops is that a load drop has lowered the stress intensity value below critical. However, the experimental observation in several investigations<sup>(1,2)</sup> have been that the load decreases little if any during pop-in. Furthermore, dead-weight loading in a creep frame has resulted in pop-in crack arrest<sup>(3)</sup> so that a load drop in itself is not a necessary condition. In considering other crack arrest mechanisms, various types of crack growth resistance<sup>(4-6)</sup> or energy<sup>(7)</sup> criteria were considered. However, these approaches did not provide enough physical behavior with which to make a complete analysis. For this reason, a simpler, although slightly less tenable, engineering approach was hypothesized.

Engineering Model

To answer the first question posed above, it was assumed that the crack stops because of an "effective" load reduction. Referring to the first schematic in Fig. 1, it is assumed that a parabolic crack front pops in to a distance  $a_0 + \ell_1$ . If an imaginary line is drawn perpendicular to the crack apex at  $a_0 + \ell_1$ , there remains the shaded area which is undergoing severe plastic deformation. The stress intensity associated with the new crack length,  $a_0 + \ell_1$ , undergoes an "effective" load relaxation provided by the shaded area. Thus the effective load would be given by

$$P_{\text{eff}} = P_{\text{actual}} - \sigma_{\text{YS}} A \quad (1)$$

if the shaded area, A, is considered to have reached the yield strength,  $\sigma_{\text{YS}}$ . In terms of the applied stress,  $\sigma$ , acting over a thickness, B, and a width, W, the effective stress becomes

$$\sigma_{\text{eff}} = \sigma - \frac{\sigma_{\text{YS}} A}{BW} \quad (2)$$

Taking a parabolic shape as indicated in Fig. 1, the shaded area is  $B\ell/3$  so that the effective stress is

$$\sigma_{\text{eff.}} = \sigma - \frac{\sigma_{\text{YS}} \ell}{3W} \quad (3)$$

At the same time the effective stress is decreasing, the crack is increasing by a length,  $\ell$ , so that the effective stress intensity for an infinite plate is given by

$$K_{\text{eff}} = \left[ \sigma - \frac{\sigma_{\text{YS}} \ell}{3W} \right] \left[ \pi(a + \ell) \right]^{1/2} \quad (4)$$

By putting the stress in terms of the stress intensity,  $K_1$ , at the start of pop-in,  $\sigma = K_1 / (\pi a)^{1/2}$ , and dividing equation (4) by  $K_1$  gives

$$\frac{K_{\text{eff}}}{K_1} = \left[ 1 - \frac{\sigma_{\text{YS}} (\pi a)^{1/2}}{3W K_1} \ell \right] \left[ 1 + \frac{\ell}{a} \right]^{1/2} \quad (5)$$

A schematic of equation (5) is shown in Fig. 2. It is significant that the effective stress intensity first increases with increasing crack length

and then decreases. It may be shown that  $K_{eff}/K_i$  becomes only slightly larger than unity and so it takes a small effective load reduction to lower  $K_{eff}$  to  $K_i$ . It is hypothesized that once  $K_{eff}$  does reduce back to  $K_i$  the crack stops and this defines the pop-in length indicated in Fig. 2. Thus, setting  $K_{eff}/K_i$  equal to unity in equation (5) allows calculation of the pop-in length from

$$l = \frac{a}{2} \left\{ \left[ 2 \left( \frac{\alpha}{a} \right) - 1 \right] - \left[ 4 \left( \frac{\alpha}{a} \right) + 1 \right]^{1/2} \right\} \quad (6)$$

$$\text{where } \alpha = \frac{3WK_i}{\sigma_{YS}(\pi a)^{1/2}}$$

Of course, for the first pop-in,  $K_i$  has been associated with  $K_{IC}$  (8), but for the purposes of generality,  $K_i$  will be taken as the stress intensity at the start of any pop-in. This is particularly useful when considering multiple pop-in data. One further description from this model is useful. As the pop-in length goes to zero, this physically describes the case where no pop-in can occur. This can be obtained by putting equation (6) into terms of stress intensity

$$K_i = \frac{\sigma_{YS}(\pi a)^{1/2} l}{3W \left[ 1 - \left( \frac{a}{a+l} \right)^{1/2} \right]} \quad (7)$$

and taking the limit

$$\lim_{l \rightarrow 0} K = \lim_{l \rightarrow 0} \frac{\sigma_{YS}(\pi a)^{1/2}}{3W \left[ \frac{1}{2a} \left( \frac{a+l}{a} \right)^{-3/2} \right]}$$

which becomes

$$K_i = \frac{2(\pi)^{1/2} \sigma_{YS} a^{3/2}}{3W} \quad (8)$$

It is significant that applied stress does not appear in equation (8). It is hypothesized that equation (8) gives a geometrical limit to pop-in behavior and for  $K$  values less than  $K_i$ , no pop-in should occur. This does not mean that pop-in has to occur at  $K_i$  defined by equation (8). Certainly,  $K_{IC}$  is a material parameter and if  $K_i < K_{IC}$  no pop-in would occur since the material criterion would not be satisfied. However, if  $K_i > K_{IC}$ , equation (8) indicates that no pop-in would occur even though  $K_{IC}$  were reached.

Now that a mathematical description of the model has been made, it is reasonable to reflect upon some of the assumptions. First, a parabolic crack shape was assumed as many metallic specimens exhibit this type of crack front, notably high strength steel, aluminum and titanium alloys<sup>(9)</sup>. Also, this shape has been observed in plastics<sup>(1)</sup> as illustrated in Fig. 3. Secondly, it is not too unrelastic to assume an initially straight cut at the start of each pop-in. This behavior, as indicated in Fig. 1(a), shows the crack front following the dashed lines until it reaches a straight cut for the second pop-in. Justification of this behavior has two bases. First, cracking between major pop-ins was detected using stress-waves as indicative of crack growth<sup>(2)</sup>. Secondly, cracking along the dashed lines might be expected prior to a second pop-in as Dixon<sup>(10)</sup> has shown the stress intensity to be highest at the outer edges of the dashed curve.

If no cracking between pop-ins occurred, the other extreme as indicated in Fig. 1(b) would result. It is seen that although conditions for the first pop-in, 1(b), are the same as in 1(a), the shaded area associated with the second pop-in, 1(b), is greater than that for the second pop-in in 1(a). Features similar to those depicted in Fig. 1(b) have been observed on fracture faces. However, this behavior cannot extend to large amounts of slow crack growth where surface cracking is noted. For this reason and the greater analytical simplicity of model 1(a), the straight cut was considered.

#### Experimental Evidence

Pop-in data from single-edge notch specimens of 7075-T6 aluminum<sup>(2)</sup> were compared to this model. A typical load-displacement curve obtained upon a 6-inch wide specimen is shown in Fig. 4. It may be noted that there are multiple pop-ins and that the pop-in length increases with load (or increasing stress intensity). A tabulation of all data from two previous investigations<sup>(1,2)</sup> is given in Table 1. Pop-in lengths were plotted as a function of initial stress intensity in Fig. 5. For comparison, calculations of  $l$  from equation (6) were made for the 3 and 6-inch wide cases and are also shown in Fig. 5. Since the crack length was increasing slightly during the test, the actual value of  $a$  was used in the calculation as taken from the experimental observations. For example, one such plot of crack length versus stress intensity is shown in Fig. 6.

Comparing the calculated and observed pop-in data in Fig. 5 make two points immediately apparent. First, both the data and the model indicate that pop-in length increases with increasing stress intensity. Secondly,

although the pop-in lengths from equation (6) are of the right order of magnitude, they are about a factor of 5 to 10 large for much of the data. The notable exception is the 0.5 inch thick data for which the model predicts pop-in length very closely. The other significant feature of Fig. 5 is the geometrical limit for pop-in as taken from equation (8). It is seen that it predicts the lower bound for pop-in reasonably well for both the 3-inch wide and 6-inch wide data. It should be pointed out that this model predicts a much lower bound for pop-in than the 1.5 inch wide data listed in Table 1. However, since  $K_{IC}$  is not exceeded at this low stress intensity, no pop-in occurs. In any case, one should not be tempted too far in this analysis since it is mostly qualitative in substance. Still, it does pose some interesting questions for further analysis of pop-in behavior.

Several comments are appropriate about the limitations of the present model. First, the above analysis applies to a crack in an infinite plate whereas the experimental data was obtained with single-edge notched specimens. The effect of geometric corrections could be included into the analysis by replacing the crack length  $a$  and the extended length  $(a + l)$  by  $a Y^2(\frac{a}{w})$  and  $(a + l) Y^2(\frac{a+l}{w})$  respectively. The factor  $Y(a/w)$  is given by Brown and Srawley<sup>(6)</sup> for various geometries including the single edge notch design. Figure 7 shows the results of including these factors for a specific specimen design. Although the curves are displaced from one another, the shape of the curves are very similar. Thus, the simpler infinite plate case was used to analyze the experimental results.

Secondly, there has been no consideration that the fracture criterion may be changing as the crack lengthens. That is, as the crack pops-in, the crack front is gradually progressing from a plane strain situation to a plane stress one. This may be expected to change the critical stress intensity for crack growth and so  $K_{eff}$  may not quite have to get back to  $K_I$  as was indicated in Fig. 2. Finally, the present model has only considered a straight crack front at the start of each pop-in. If the extreme of Fig. 1(b) had been used instead of 1(a), an entirely different pop-in behavior would have been predicted. In fact, except for the first pop-in, no others would occur. This indicates that the crack shape could vary the pop-in length from zero to the predicted value given by equation (6). Thus, a model could probably be picked between the extremes shown in Fig. 1 to approximate the observed crack lengths. Experimental evidence for this is given by Dixon<sup>(10)</sup> where the crack shape at the start of a second or third pop-in is definitely between the extremes indicated in Fig. 1.

One final point of encouragement was obtained for the present model. In the one pop-in value listed in Table 1 for Lexan plastic, a large pop-in of 0.101 inches was associated with an initially straight crack front. Utilizing the finite width analysis as depicted in Fig. 7, a calculated pop-in of 0.115 inches is obtained which is very close to the observed value. In connection with this calculation, it should be noted that the yield strength is 8500 psi. Thus far, the questions of why a pop-in stops and how far will it lengthen have been considered. It is now appropriate to consider the last two questions posed in the Introduction which deal with multiple pop-in behavior.

#### MULTIPLE POP-IN CONSIDERATION

Referring back to Fig. 4, it is seen that multiple pop-ins exist and that there seems to be a stress-intensity increment between each pop-in. Why it takes an additional stress to trigger the next pop-in may be explained in part by a changing fracture criterion. That is, with an increase in load and crack length, a greater percentage of the thickness at the crack front will be under plane stress conditions. Also, with increasing stress intensity, the crack tip blunts which can also raise the fracture criterion. The engineering model is based upon these two considerations.

#### Engineering Model

A changing fracture criterion may be taken into account by assuming a simple addition of the failure criterions which apply separately to the plane stress and plane strain portions of the crack front. This can be visualized by the following word equation

$$\{\text{Plane Stress Criterion}\}\{\text{Plastic Zone}\} + \{\text{Plane Strain Criterion}\}\{\text{B-Plastic Zone}\} = \{\text{POP-IN}\} \quad (9)$$

This assumes that the plane stress criterion applies to the plastic zone at the surface. For a circular plastic zone extending from both surfaces to a depth equal to the plastic zone radius, the amount of material involved in plastic deformation would be  $K_n^2 / 3\pi \sigma_{ys}^2$  at an applied stress intensity of  $K_n$ . For the plane stress and plane strain criterions, the crack tip displacement is used so that compatibility with the crack-tip blunting analysis is achieved. Noting that the crack-tip displacement is proportional to the square of the stress intensity, equation (9) may be written as

$$K_{IC}^2 \left[ \frac{K_n^2}{3\pi \sigma_{ys}^2} \right] + K_{I0}^2 \left[ 1 - \frac{K_n^2}{3\pi \sigma_{ys}^2} \right] = K_{I0}^2 \quad (10)$$

The physical interpretation of this equation is that at  $K_n$  the crack has popped in. The fracture criterion changes due to the change in the plastic zone and now it requires a new stress intensity level,  $K_{n+1}$ , for the  $n_{th+1}$  pop-in. Since  $K_{n+1}$  can be described by

$$K_{n+1} = K_n + \Delta K_{n+1} \quad (11)$$

the stress intensity increment required for the  $n_{th+1}$  pop-in may be found from equations (10) and (11) to be

$$\Delta K_{n+1} = \left[ \frac{K_{IC}^2 E \pi \sigma_{YS}^2 - K_{IC}^2 K_n^2 + K_c^2 K_n^2}{E \pi \sigma_{YS}^2} \right]^{1/2} - K_n \quad (12)$$

The first pop-in would occur at  $K_n = K_{IC}$  so that all quantities are known in equation (12) to determine  $\Delta K_{n+1}$  for the second pop-in. Once this has been calculated, it defines  $K_{n+1}$  from equation (11) and a calculation of the third pop-in may be made.

Besides this changing fracture criterion, there is also the effect of crack tip blunting to be considered. E. Smith<sup>(11)</sup> has extended the B.C.S.<sup>(12)</sup> model to blunt cracks and has shown that blunting the crack changes the displacement criterion in front of the crack. He finds the crack tip displacement,  $v_c$ , to be a function of crack tip radius,  $\rho$ ,

$$v_c = \frac{4\sigma_{YS}a}{\pi E} \ln \left[ \sec \frac{\pi}{2} \left\{ \frac{\sigma}{\sigma_{YS}} - \left( \frac{\rho}{a} \right)^{1/2} \left( 1 - \frac{\sigma}{\sigma_{YS}} \right) \right\} \right] \quad (13)$$

It may be noted that this relationship reduces to Goodier and Field's<sup>(13)</sup> result for  $\rho \rightarrow 0$ . The crack tip radius can be approximately described according to Tetelman<sup>(14)</sup> by

$$\rho \approx \frac{v_c}{\epsilon^*} \quad (14)$$

where  $\epsilon^*$  is the fracture strain. Furthermore, the crack-tip displacement can be approximately described in terms of the stress intensity by<sup>(15)</sup>

$$v_c \approx \frac{K^2}{2\sigma_{YS}E} \quad (15)$$

With equations (14) and (15), a new parameter, Z, is defined as  $\rho/a$  and is given by

$$Z = \rho/a \approx \frac{v_c}{\epsilon^* a} \approx \frac{K_n^2}{2\sigma_{ys} E \epsilon^* a_n} \quad (16)$$

Three additional considerations to the crack-tip blunting analysis are made as follows. First, the changing fracture criterion analogous to that in equation (10) for crack-tip displacements is made. Secondly, an approximation to the  $\ln[\sec \theta]$  is made from the first term of the trigonometric expansion to be  $\frac{\theta^2}{2}$ , where  $\theta$  is the rest of the right hand side of equation (13) starting with  $\frac{\pi}{2}$ . Thirdly, the applied stress is put in terms of stress intensity as was done before for equation (5). These three considerations along with equations (13) and (16) lead to

$$K_{IC}^2 \left[ 1 - \frac{K_n^2}{B\pi\sigma_{ys}^2} \right] + K_c^2 \left[ \frac{K_n^2}{B\pi\sigma_{ys}^2} \right] = \{ K_{n+1} [Z^{1/2} + 1] - \sigma_{ys} [\pi a_n Z]^{1/2} \}^2 \quad (17)$$

From equations (11) and (17), the stress intensity increment for the  $n_{th+1}$  pop-in becomes

$$\Delta K_{n+1} = \frac{\{ K_{IC}^2 \left[ 1 - \frac{K_n^2}{B\pi\sigma_{ys}^2} \right] + K_c^2 \left[ \frac{K_n^2}{B\pi\sigma_{ys}^2} \right] + \sigma_{ys} [\pi a_n Z]^{1/2} \}^{1/2}}{1 + Z^{1/2}} - K_n \quad (18)$$

Appropriately, equation (18) reduces to equation (12) for  $n$  infinitely sharp crack, i.e., as  $Z \rightarrow 0$ . It is now suitable to compare equations (12) to the experimental data.

#### Experimental Evidence

In order to compare the model to the experimental evidence, three factors had to be described -  $K_{IC}$ ,  $K_c$  and  $Z$ . The yield strength was already known to be 78 Ksi for this heat of 7075-T6 aluminum<sup>(2)</sup>.  $K_{IC}$  was taken as 28 Ksi-in<sup>1/2</sup> as this was the lowest stress intensity at which pop-in was obtained. This is also not unreasonable compared to other experimental data<sup>(16)</sup>.  $K_c$  was taken as 55 Ksi-in<sup>1/2</sup> since this was the average value of  $K$  at instability in those tests where plane stress failure was observed. Finally,  $Z$  is defined by known parameters in equation (16) except for the fracture strain,  $\epsilon^*$ , which was measured from uniaxial data to be 0.30.

An example of the calculation technique using equation (18) is given in Table 2. Using the above values,  $\Delta K_1$  was determined from equation (18) for  $K_n = 45.7 \text{ Ksi-in}^{1/2}$  at which the first pop-in occurred in the 6-inch wide plate. This gives a value of  $2.3 \text{ Ksi-in}^{1/2}$  for  $\Delta K_1$  and so the second pop-in from equation (11) would be at  $48.0 \text{ Ksi-in}^{1/2}$ . Similarly, the next stress intensity increment  $\Delta K_2$  to the third pop-in was calculated to be  $1.5 \text{ Ksi-in}^{1/2}$ . As indicated in Table 2, this procedure gives values of  $\Delta K$  for the first three increments that are comparable to those observed. However, the last two are not very close in agreement. Nevertheless, the fact that multiple pop-ins are predicted and that, quantitatively, they are the right order of magnitude is encouraging.

Similar calculations for  $\Delta K$  from equations (12) and (18) were made for the case of  $B = 0.25$  inches and  $a = 1.0$  inch starting at  $K_{IC}$ . In Fig. 8, the two resulting curves were then compared to all of the 0.25 inch data from Table 1. Regardless of crack length or specimen width, all of the data may be compared on the same plot to equation (12) since it is independent of  $a$  and  $W$ . This is not quite the case for equation (18) since crack length appears and  $Z$  is a function of crack length. However, as  $Z$  is proportional to  $\frac{1}{a}$ , the term in the numerator is independent of  $a$ . Furthermore, since  $Z^{1/2}$  is small compared to unity, equation (18) is nearly independent of crack length. Thus, for practical purposes, all of the data are compared in Fig. 8. It is seen that equation (12) underestimates the stress intensity increment required for the next pop-in. Incorporation of the crack-tip blunting effects in equation (18) gives a reasonable comparison to the data. Although the calculated curves are somewhat steeper in slope than the data, the model does predict the downward trend of  $\Delta K$  with increasing stress intensity and the magnitudes of  $\Delta K$  are remarkably close to those observed.

#### Transitional Fracture Behavior

One further physical phenomenon may be examined with this approach. As the crack pops in at higher and higher stress intensity levels, there is a gradual fracture mode transition. Thus, one might expect that equation (18) could be used to examine the thickness effect on fracture toughness. As  $\Delta K$  goes to zero, no additional stress intensity is required to propagate a crack. Physically, then, one might interpret the point at which  $\Delta K$  goes to zero as the critical stress intensity factor for fracture instability. The limit of equation (18) as  $\Delta K \rightarrow 0$  is given by

$$K_n [1 + Z^{1/2}] - \sigma_{ys} (\pi a_n Z)^{1/2} - \left\{ K_{IC}^2 \left[ 1 - \frac{K_n^2}{B\pi\sigma_{ys}^2} \right] + K_c^2 \left[ \frac{K_n^2}{B\pi\sigma_{ys}^2} \right] \right\}^{1/2} = 0 \quad (19)$$

If the physical interpretation is correct, then  $K_n$  in equation (19) is  $K_{CB}$  for a given thickness. This should not be confused with the  $K_c$  value given in equation (19) which is the experimentally observed value for 100 percent plane stress failure. Setting  $K_{CB} = K_n$  gives the critical stress intensity for any mixed mode failure, i.e., any thickness. Values of  $K_{CB}$  were determined from equation (19) using  $K_{IC} = 28 \text{ Ksi-in}^{1/2}$  and  $K_c = 55 \text{ Ksi-in}^{1/2}$  as before and considering a one-inch long crack. This is shown in Fig. 9 along with the experimentally observed values of  $K_{CB}$ . Only two values were available from the present analysis but additional data from Kaufman and Hunsicker<sup>(16)</sup> were available for the identical alloy and condition. The agreement is surprisingly good.

The lower bound indicated in Fig. 9 is obtained by calculating the thickness at which  $K_n = K_c$  in equation (19). This also makes mathematical sense as the solution diverges for  $K_n > K_c$ . In this way the lower bound for mixed mode failure was determined to occur at a thickness of 0.23 inches. Thus, not only can multiple pop-in data be interpreted, but also a tentative explanation of fracture-mode transition is obtained. Again, it should be emphasized that these are infinite plate analyses and so the indicated effect of crack length may not be realistic for finite width plates.

CONCLUSIONS

1. Experimentally, both pop-in length and the stress intensity increment between multiple pop-ins vary with stress intensity factor.
2. Semi-quantitative models to account for both of these effects are derived;

a) For pop-in length,  $l$ ,

$$l = \frac{a}{2} \left\{ \left[ 2 \left( \frac{\alpha}{a} \right) - 1 \right] - \left[ 4 \left( \frac{\alpha}{a} \right) + 1 \right]^{1/2} \right\}$$

where  $\alpha$  depends upon stress intensity, width, yield strength and crack length. This predicts pop-in length to increase with increasing stress intensity as is the experimental observation.

b) For the stress intensity increment between multiple pop-ins,  $\Delta K$ ,

$$\Delta K_{n+1} = \frac{\left\{ K_{IC}^2 \left[ 1 - \frac{K_n^2}{B\pi\sigma_{ys}Z} \right] + K_C^2 \left[ \frac{K_n^2}{B\pi\sigma_{ys}Z} \right] \right\}^{1/2} + \sigma_{ys} [\pi a_n Z]^{1/2}}{1 + Z^{1/2}} - K_n$$

where the K's are stress intensities, B is the thickness and Z is a factor dependent upon variation in the crack tip radius due to blunting. This predicts  $\Delta K$  to decrease with increasing stress intensity and is confirmed by the experimental observations.

3. As  $l \rightarrow 0$ ,

$$K_i = \frac{2\sigma_{ys}(\pi)^{1/2} a^{3/2}}{3W}$$

which is tentatively hypothesized to be a geometrical lower bound for pop-in. That is, pop-in occurs at  $K_{IC}$  only if

$$K_{IC} \geq K_i$$

4. As  $\Delta K > 0$ , the above equation in conclusion 2 (b) is used to interpret the fracture mode transition. The critical stress intensity factor is shown to be a function of thickness and the proposed relationship is in good agreement with two sets of experimental data.

REFERENCES

1. P. L. Key and Y. Katz, "On the Pop-In Mode of Fracture," Submitted to International Journal of Fracture Mechanics, January 1968.
2. C. E. Hartbower, W. W. Gerberich and H. Liebowitz, J. of Eng. Fracture Mechanics, Vol. 1, No. 2, April 1968.
3. C. E. Hartbower, W. W. Gerberich and P. P. Crimmins, "Mechanisms of Slow Crack Growth in High Strength Steels," AFML TR-67-26, Vol. 1, February 1967.
4. G. R. Irwin, "Fracture Testing of High Strength Sheet Materials Under Conditions Appropriate for Stress Analysis," NRL Report 5486, July 27, 1960.
5. J. M. Krafft, A. M. Sullivan and R. W. Boyle, Proc. Crack Propagation Symp., Cranfield England, Vol. 1, 1961, p.8.
6. J. E. Srawley and W. F. Brown, Jr., Fracture Toughness Testing and its Applications, ASTM Spec. Tech. Pub. 381, 1965, p. 133.
7. D. Broek, "The Residual Strength of Cracked Sheet and Structures," National Aero-and Astronautical Research Institute, Amsterdam, NLR-TM-M 2135, August 1964.
8. R. W. Boyle, A. M. Sullivan and J. M. Krafft, Welding J. Res. Supp., September 1962, p. 428-S.
9. C. E. Hartbower, W. W. Gerberich, W. G. Reuter and P. P. Crimmins, "Stress-Wave Characteristics of Fracture Instability in Constructional Alloys," Contract N00014-66-C0340, Office of Naval Research, August 1967.
10. J. R. Dixon, "Effects of Crack-Front Geometry and Plate Thickness on the Stress Distribution in Cracked Plates," Proc. Conf. on Phys. Basis of Yield and Fracture,
11. E. Smith, Proc. Roy. Soc. London, Vol. 299A, No. 1459, July 1967, p.455.
12. B. A. Bilby, A. H. Cottrell, and K. H. Swinden, Proc. Roy. Soc. London, Vol. 272A, 1963, p. 304.
13. J. N. Goodier and F. A. Field, Fracture of Solids, Ed. by Drucker and Gilman, Interscience, New York, 1963, p. 103.
14. A. S. Tetelman and A. J. McEvily, Fracture of Structural Materials, John Wiley and Sons, New York, 1967.

15. G. T. Hahn and A. R. Rosenfield, Acta Metallurgica, Vol. 13, March 1965, p. 293.
16. J. G. Kaufman and H. Y. Hunsicker, Fracture Toughness Testing and Its Applications, ASTM STP 381, 1965, p. 290.

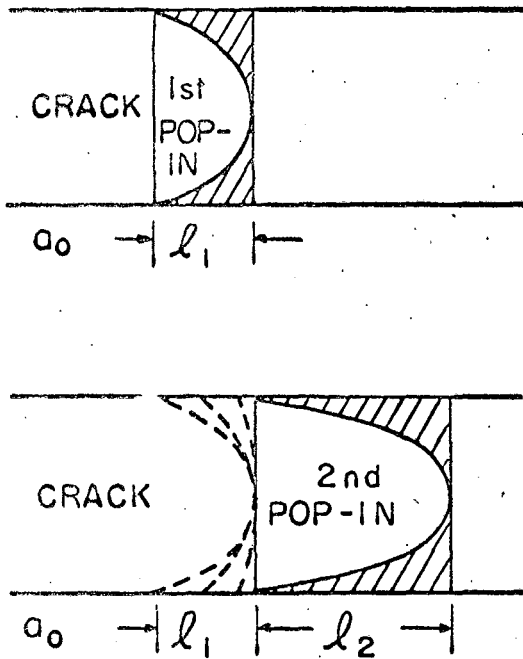
Table 1. Summary of Pop-in Data

Specimen Number	Material	Thickness	Width	Crack Initial	Length Final	K <sub>i</sub> at Pop-in ksi(in) <sup>1/2</sup>
		in.	in.	in.	in.	
75-10	7075-T6	.50	3.0	.927	.935	27.5
				.939	.957	28.8
				.969	1.060	32.6
				1.062	1.150	39.5
75-11	7075-T6	.25	3.0	.971	.990	31.3
				.994	1.022	36.9
				1.045	1.089	43.2
				1.098	1.151	49.1
75-21	7075-T6	.25	3.0	1.118	1.151	46.0
75-20	7075-T6	.25	3.0	.602	.619	29.0
				.631	.635	36.2
				.646	.661	41.0
				.673	.728	44.8
75-1	7075-T6	.25	1.5	.496	.501	30.1
				.504	.510	35.2
				.517	.539	40.8
				.540	.564	44.8
75-3	7075-T6	.25	6.0	1.875	1.878	45.7
				1.885	1.895	48.6
				1.896	1.917	51.4
				1.920	1.956	52.8
				1.962	2.019	54.8
				2.055	2.140	61.9
	Lexan	.25	1.0	.342	.443	3.1

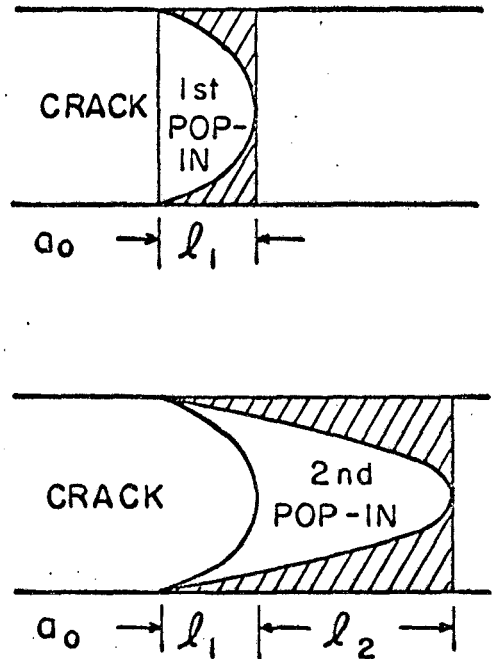
Note: All specimens were single edge notch type.

Table 2. Comparison of calculated and observed stress intensity increments between "pop-ins".

Specimen	Calculated		Observed	
	K, Ksi-in <sup>1/2</sup>	$\Delta K$ , Ksi-in <sup>1/2</sup>	K, Ksi-in <sup>1/2</sup>	$\Delta K$ , Ksi-in <sup>1/2</sup>
75-3	45.7	2.3	45.7	2.9
W = 6	48.0	1.5	48.6	2.8
a = 2	49.5	1.0	51.4	1.4
B = 0.25	50.5	0.6	52.8	2.0
	51.1	0.4	54.8	7.1



a. CONSIDERING STRAIGHT CRACK AT THE START OF EACH POP-IN.



b. CONSIDERING CURVED CRACK FRONT ANCHORED AT SURFACE.

Fig. 1 Schematics depicting two possibilities of multiple pop-in behavior

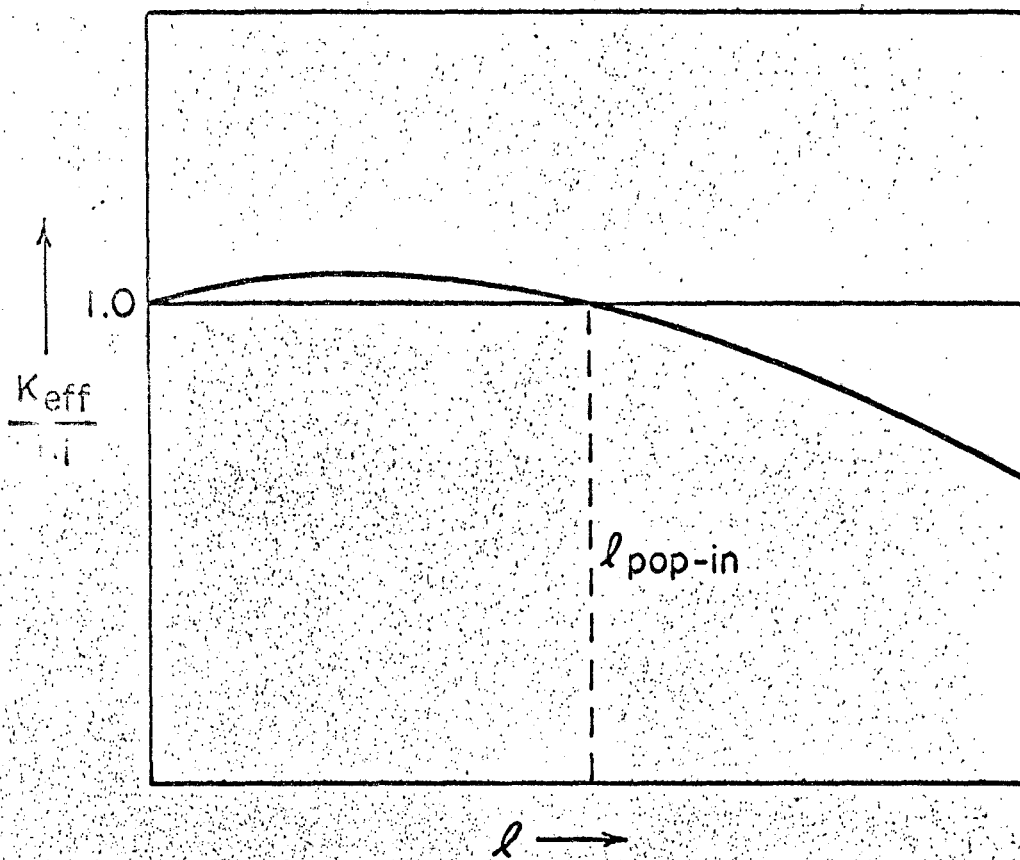


Fig. 2. Schematic of Equation (5)



XBB 6711-6445-A

Fig. 3 Pop-in in Lexan (polycarbonate) plastic.

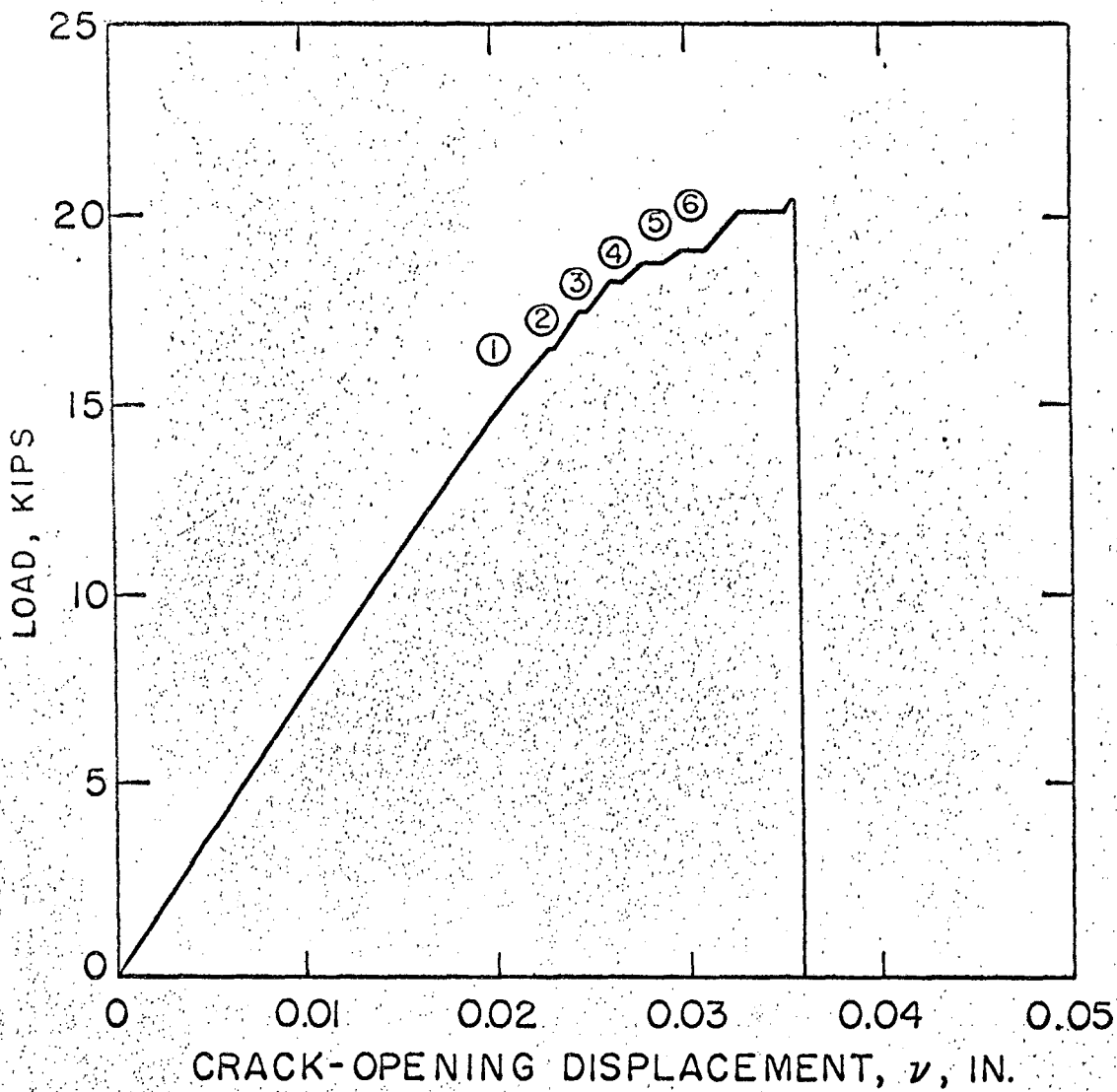


Fig. 4 Load displacement curve showing multiple pop-ins in 6 in. wide 7075-T6 aluminum specimen.

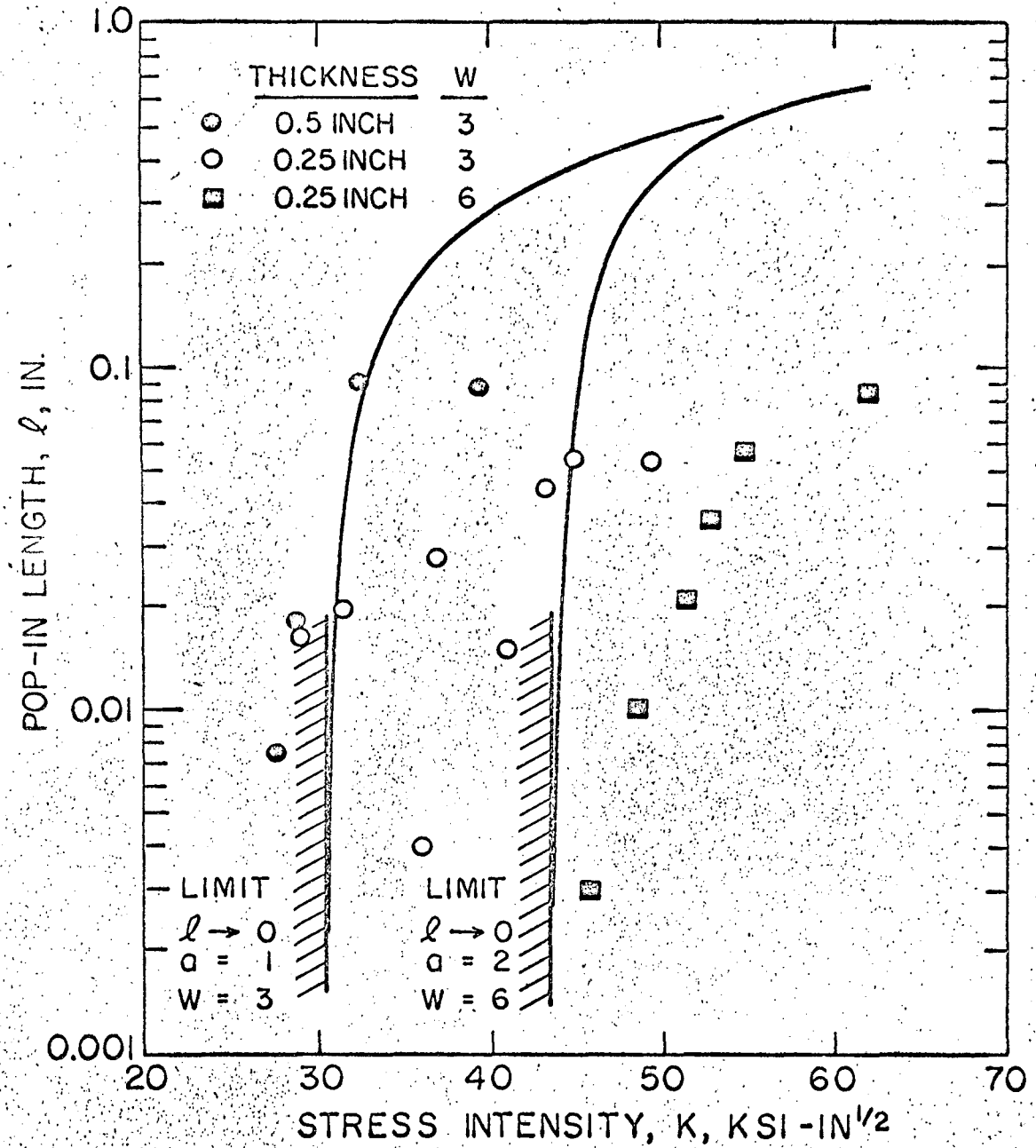


Fig. 5. Effect of applied stress intensity on pop-in length: calculated, Eq. (6), and observed.

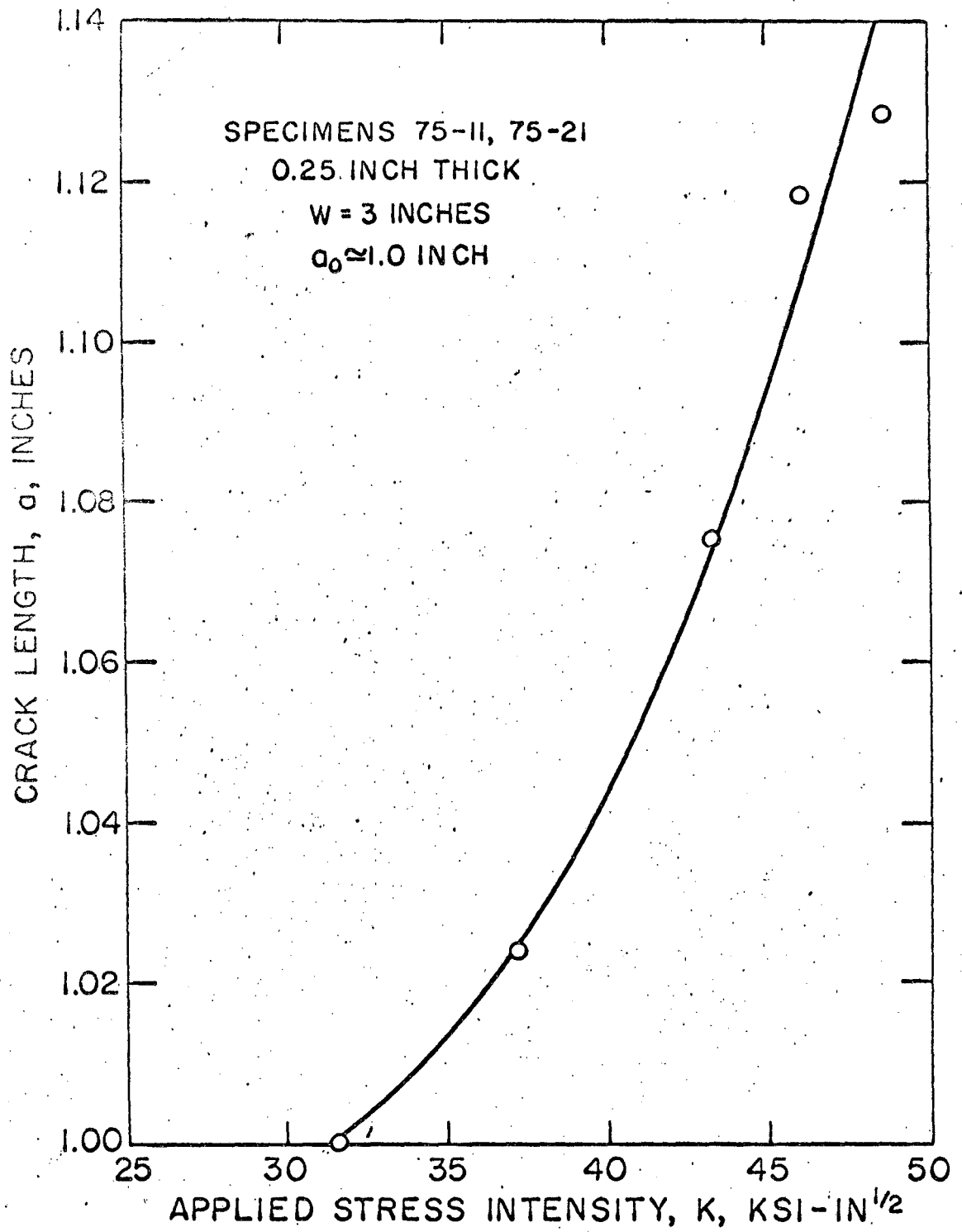


Fig. 6 Increase of crack length with applied stress intensity.

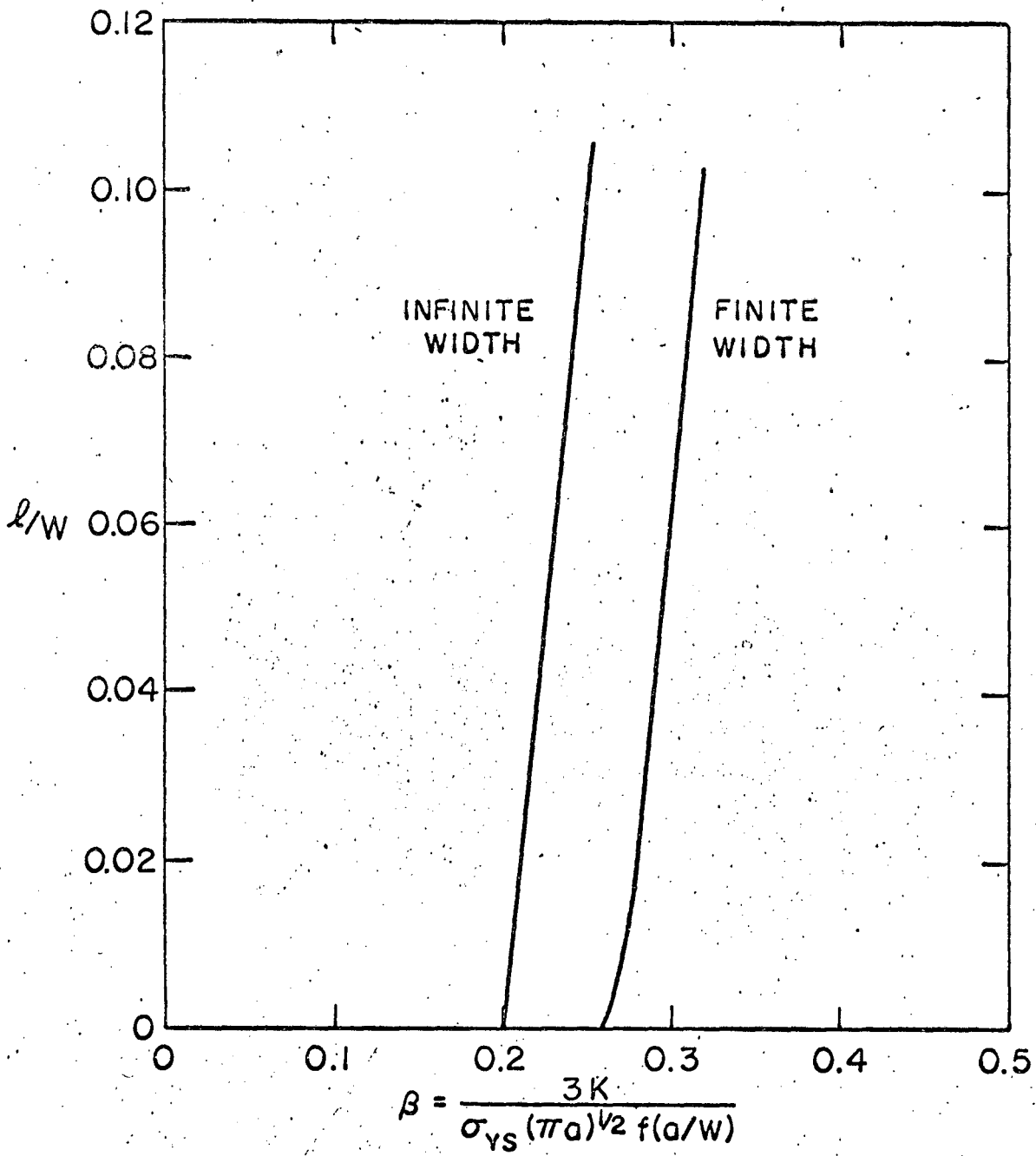


Fig. 7 Comparison of infinite width and finite width analyses.

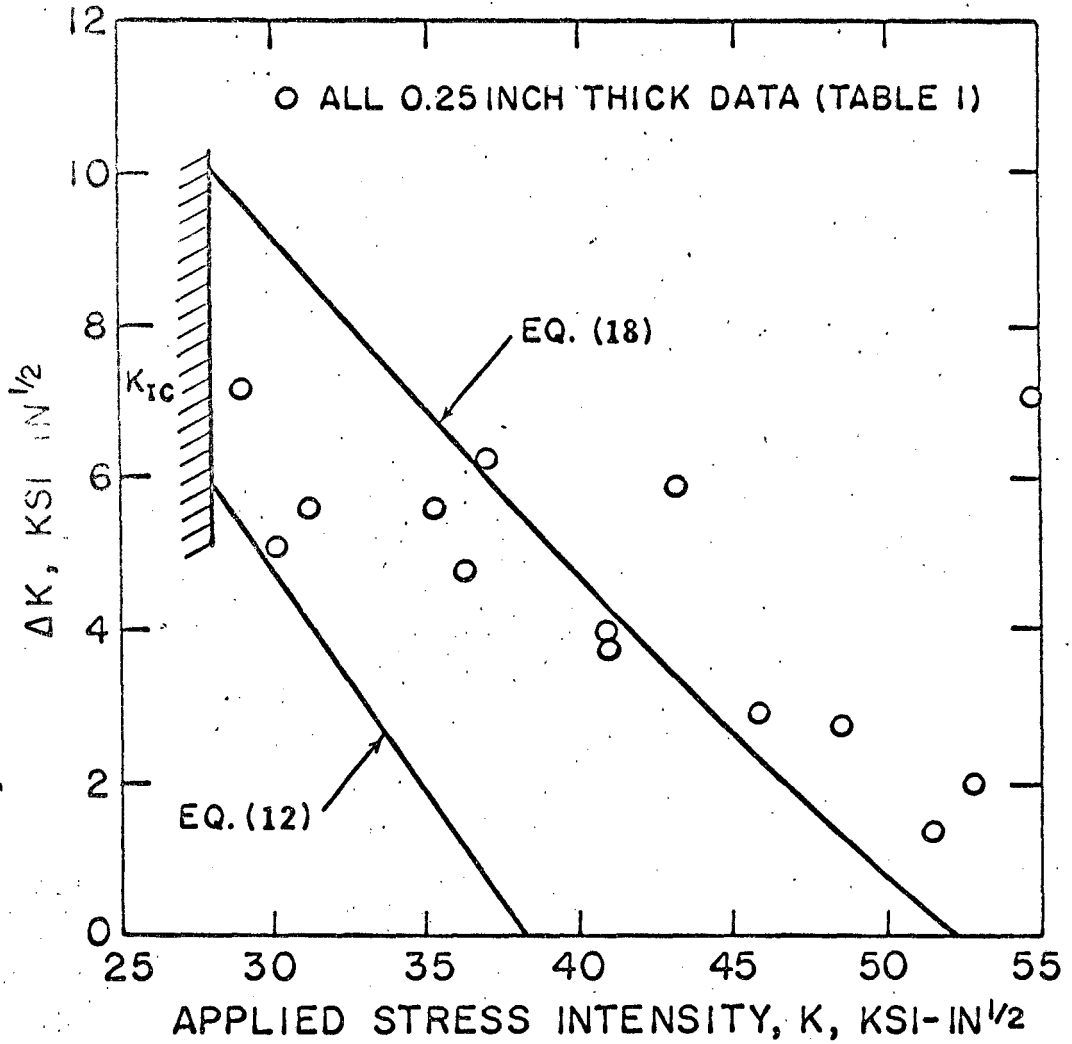


Fig. 8 Effect of applied stress intensity on increments between pop-ins: calculated and observed.

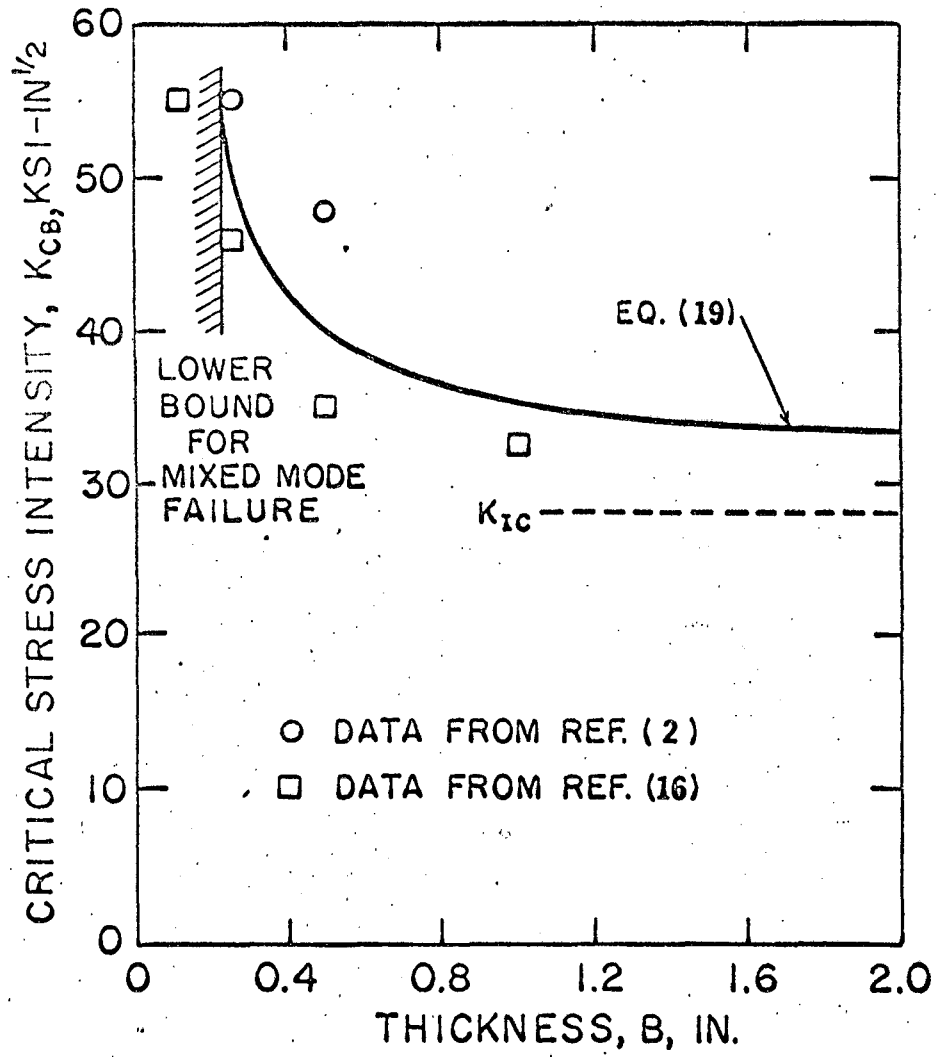


Fig. 9 Comparison of calculated and experimental fracture mode transition.

This report was prepared as an account of Government sponsored work. Neither the United States, nor the Commission, nor any person acting on behalf of the Commission:

- A. Makes any warranty or representation, expressed or implied, with respect to the accuracy, completeness, or usefulness of the information contained in this report, or that the use of any information, apparatus, method, or process disclosed in this report may not infringe privately owned rights; or
- B. Assumes any liabilities with respect to the use of, or for damages resulting from the use of any information, apparatus, method, or process disclosed in this report.

As used in the above, "person acting on behalf of the Commission" includes any employee or contractor of the Commission, or employee of such contractor, to the extent that such employee or contractor of the Commission, or employee of such contractor prepares, disseminates, or provides access to, any information pursuant to his employment or contract with the Commission, or his employment with such contractor.

